Current Research in Green and Sustainable Chemistry 5 (2022) 100303

Contents lists available at ScienceDirect

Current Research in Green and Sustainable Chemistry

journal homepage: www.elsevier.com/journals/current-research-in-green-and-sustainable-chemistry/2666-0865

Biosynthesis of selenium nanoparticles using combinations of plant extracts and their antibacterial activity

Lucas Marcelino dos Santos Souza [a], Miriam Dibo [a], Juan Josue Puño Sarmiento [a], Amedea Barozzi Seabra [b], Leonardo Pinto Medeiros [a], Isabella Martins Lourenço [b], Renata Katsuko Takayama Kobayashi [a], Gerson Nakazato [a,*]

[a] Department of Microbiology, Biological Sciences Center, State University of Londrina (UEL), Londrina, Paraná, Brazil, University Campus, PR, CP 86057-970
[b] Center for Natural and Human Sciences (CCNH), Federal University of ABC (UFABC), Santo André, São Paulo, CP 09210-580, Brazil

ARTICLE INFO

Keywords:
Nanotechnology. plants. antimicrobial. cytotoxicity

ABSTRACT

Antimicrobial resistance is a significant public health problem, and the use of nanotechnology to control bacterial growth has increased, including multidrug-resistant ones. In this context, nanoparticles of different elements, mainly metals, such as silver, gold, and iron, have been extensively researched due to their efficient antimicrobial activity. Another element that stands out is selenium, which nanoparticles have high bioactivity and antibacterial action, although few studies report its use as a metallic nanoparticle. Therefore, the objective of this study was to perform the synthesis of selenium nanoparticles (SeNPs) from extracts of three plants: *Allium cepa* (onion), *Malpighia emarginata* (acerola), and *Gymnanthemum amygdalinum* (boldo). The synthesized nanoparticles were characterized by Dynamic Light Scattering (DLS), scanning electron microscopy (SEM), Fourier-Transform Infrared Spectroscopy (FTIR) and X-Ray Diffraction (DRX). Antibacterial activity was evaluated by microdilution in broth, followed by the time-kill curve analysis. The bacterial strains tested were *Streptococcus agalactiae*, *Staphylococcus aureus*, methicillin-resistant *S. aureus*, *Pseudomonas aeruginosa*, and *Escherichia coli*. Hemolytic activity was also determined. The synthesized SeNPs had a size between 245 and 321 nm and mostly spherical morphology. Antimicrobial activity against all Gram-positive bacteria tested was observed, with minimal inhibitory concentrations ranging from 6.125 to 98 μg/ml, but without action in the tested Gram-negative bacteria. Low hemolytic capacity was observed, with CC_{50} ranging from 0.82 to 2.1 mg/ml. The antimicrobial activity and low hemolytic concentration indicate the possibility of use against Gram-positive bacteria, including multidrug-resistant ones, opening a wide variety of options for their applications.

1. Introduction

Antimicrobial-resistant bacteria are a significant concern and have become a global and highly complex problem. Some consequences of this problem are the difficulty and increased cost of treatment, and an increase in the mortality and morbidity rates of those affected, harming the economy and health sectors. The measures related to its solution consist in the development of compounds and alternative therapies, in addition to awareness policies to the rational use of antibiotics, epidemiological studies of antimicrobial resistance, and monitoring of multidrug-resistant bacteria (MDR) cases [1]. Therefore, a great alternative to combat this problem is producing new therapies, with natural origin and nanotechnology-related compounds, such as biological nanoparticles of silver, gold, and selenium, with antimicrobial properties [2–4].

Selenium can play many roles in industry as part of electronic components, solar cells, sensors, bioimaging, metallurgy, glass production, and pigment manufacturing [5,6]. Selenium is also an essential micronutrient for animal metabolism, which participates in antioxidant pathways, increases immune system function, and improves thyroid function against heart diseases [7]. This compound also participates in the neutralization of heavy metals by directly binding to its ions, preventing them from causing damage to healthy cells [8]. The recommended daily intake of selenium is 300 μg/day; however, its therapeutic window is low, and intake above 950 μg/day is considered toxic [9].

In the biomedical area, selenium can be used in patients with diabetes due to its good antioxidant function in the body, acting as an anti-inflammatory and consequently reducing the action of oxidizing agents [10,11]. Selenium can also be applied in the destruction of cancer cells

* Corresponding author.
E-mail addresses: gnakazato@uel.br, gersonakazato@yahoo.com.br (G. Nakazato).

https://doi.org/10.1016/j.crgsc.2022.100303
Received 11 November 2021; Received in revised form 22 March 2022; Accepted 27 March 2022
Available online 29 March 2022

due to its great affinity for internalization and can act as a drug delivery system [7]. Inside the cell, selenium alters the chemical properties of the cell membrane and induces the production of signaling molecules of apoptosis, leading the cancer cell to death [12].

Selenium can also acquire characteristics of nanoparticles (SeNPs). Nanoparticles have physicochemical characteristics that are distinct from the element on a macro scale, such as melting point, electrical/thermal conductivity, and light absorption, enabling their use in numerous fields of science [13].

SeNPs can be produced by chemical, physical, or biological methods and their physicochemical characteristics depend on the methodology used [14]. Chemical synthesis uses chemical reagents to reduce precursor ions present in the salt and stabilize the produced nanoparticles. It is a fast method with low differences between the manufactured batches; however, production or disposal of toxic products to the environment may occur. Physical synthesis does not use chemical reagents but requires expensive equipment and great energy expenditure. Pulsed laser ablation is an example of physical synthesis [15]. Biosynthesis, biological or green synthesis, is produced mainly by bacteria, fungi, and plant extracts. It is less toxic than chemical synthesis and is considered eco-friendly due to the absence of toxic waste production. However, the fidelity rate between batches may vary due to differences in the composition of biological agents on different occasions.

Regarding biological synthesis, many microorganisms can be used to obtain SeNPs, such as *Bacillus megaterium*, *Bacillus subtilis*, *Bacillus cereus*, *Aspergillus terreus*, *Enterococcus faecalis*, and countless others [16–18]. Microorganisms capable of synthesizing nanoparticles use several enzymes that determine different morphological characteristics of the SeNPs, resulting in complex and exclusive nanoparticles, which are often impossible to be achieved through chemical synthesis [19]. Biological synthesis may also occur using plant extracts, which showed some advantages over the others since it does not require special conditions such as the cultivation of microorganisms, sophisticated equipment, or toxic reagents. Some plants with the potential ability for nanoparticle synthesis are onion, boldo, and acerola.

Allium cepa (onion) has large amounts of quercetin, a polyphenolic flavonoid with antioxidant, anti-inflammatory, anticarcinogenic, and antimicrobial activity [20]. Previous studies have already reported the use of onion extract for the synthesis of metal nanoparticles [21]. Gomaa [22] biosynthesized silver nanoparticles with aqueous onion extract and found antibacterial activity against Gram-positive and negative bacteria. Jini, Sharmila [23] synthesized silver nanoparticles and tested their antidiabetic activity, proving to be an alternative for treating the disease.

Gymnanthemum amygdalinum, also known as boldo baiano, belongs to the Asteraceae family. Its pharmacological activities are mainly attributed to the presence of saponins, tannins, alkaloids, phenolic compounds, and flavonoids [24]. Regarding its antibacterial activity, some studies analyzed the action of ethanolic and methanolic extracts of boldo leaves against Gram-positive and negative bacteria. The results showed better activity against *Staphylococcus aureus*, with minimal inhibitory concentrations (MICs) of 10 and 5 mg/ml for each extract, respectively [25,26]. However, despite the broad spectrum of boldo baiano applications, there are, to date, no studies regarding its use as an extract for the synthesis of metallic nanoparticles.

Malpighia emarginata, known as acerola, is one of the fruits with the highest content of ascorbic acid, ranging from 1 to 3% of the pulp matter [27]. Acerola's compounds have antioxidant activity, mainly due to ascorbic acid, in addition to anti-inflammatory activity, which decreases the risk of vascular diseases and prevents diseases [28]. The synthesis of nanoparticles using acerola extracts was described by Andualem [29], who synthesized copper oxide nanoparticles and reported their antibacterial activity against *S. aureus* and *Escherichia coli*.

Concerning antimicrobial activity, SeNPs demonstrate relevant action against *S. aureus* [2]. Khiralla and El-Deeb [30] showed that SeNPs produced with *Bacillus licheniformis* supernatant had action against six foodborne pathogenic bacteria, such as *B. cereus*, *E. faecalis*, *S. aureus*, *E. coli* O157:H7, *Salmonella enterica* serovar Typhimurium, and *S. enterica* serovar Enteritidis. Studies performed with SeNPs stabilized with quercetin and acetylcholine also showed great antimicrobial activity against *S. aureus* and *E. coli* [31].

Given the advantages of carrying out green synthesis to produce nanoparticles and the antibacterial activity demonstrated by SeNPs against some bacterial strains, SeNPs can be a promising alternative in searching for new antimicrobials. Therefore, the objective of this study was to synthesize green SeNPs with different plant extracts and evaluate their antibacterial activity.

2. Materials and methods

2.1. Preparation of extracts

Three species of plants, *M. emarginata* (acerola), *A. cepa* (onion), and *G. amygdalinum* (boldo), were used. Acerola pulp (100 g) (Polpasul) and red onion (200 g) were commercially purchased at a local market. The boldo leaves were harvested at the coordinates Lat: −23.2899359, Lon: -51.2439485, and identified by the herbarium of the State University of Londrina (UEL); A voucher specimen was deposited in the herbarium of the institution with the registration number 56265, washed in distilled water, and dried for 1 h. Three hydroalcoholic extracts were produced with 80% (v/v) ethanol (Merck®), one for each mentioned plant. Acerola pulp and onion bulb were added in the 100 g to 100 ml proportion, while boldo leaf was added in 25 g–100 ml of hydroalcoholic solution. The plants were crushed in a blender and extracted by maceration for 48 h, stirring every 24 h. Subsequently, the extracts were filtered on 0.22 μm filter paper (MF-Millipore®) and stored at 4 °C to carry out the tests.

2.2. Biosynthesis of SeNPs

Sodium selenite (Na_2SeO_3 - Alphatec®) was purchased as a selenium precursor. A 0.3 M sodium selenite stock solution was made with distilled water, filtered through a 0.22 μm filter, and stored at 4 °C. Four syntheses were carried out at concentrations of 10 and 20 mM with two combinations of extracts (boldo + acerola and onion + acerola), named: b10a and b20a (boldo + acerola at 10 and 20 mM, respectively), c10a, and c20a (onion + acerola at 10 and 20 mM, respectively). The sodium selenite stock solution was added to the extracts (boldo + onion) at a final concentration of 10 or 20 mM and stirred for 30 s. Then, acerola extract was gradually added in a 1:1 proportion with the solution, the pH was adjusted to 7.0, and the solution was incubated at 30 °C for six days.

2.3. Characterization of nanoparticles

2.3.1. Scanning electron microscopy (SEM)

Morphology and size verification was performed using SEM. Samples of the synthesized SeNPs were diluted in deionized water at a concentration of 1 mM, 10 μl aliquots were placed on slides coated with polylysine (1%) and allowed to dry. Subsequently, they were fixed with 0.1 M sodium cacodylate buffer solution (Merck®) (pH 7.2), 2% glutaraldehyde (Sigma-Aldrich®), and 2% paraformaldehyde (Merck®) for 20 h and posfixed with 1% tetroxide of osmium (Merck®) for 2 h. After that, the slides were exposed to increasing ethanol concentrations (70, 80, 90, and 100 °GL) for dehydration. Posteriorly, they were subjected to dehydration by critical point with CO_2 (BALTEC CPD 030 Critical Point Dryer), covered with gold (BALTEC SDC 050 SputterCoate), and analyzed in SEM (FEI Quanta 200).

2.3.2. Zeta potential and polydispersity index

The zeta potential and polydispersity index (PDI) were performed by Dynamic Light Scattering (DLS), the samples (b10a, b20a, c10a and c20a) were sent to the Federal University of ABC (Santo André – São Paulo, Brasil), and analyzed on the ZetaSizer Nano ZS (Malvern®).

2.3.3. Fourier-Transform Infrared Spectroscopy (FTIR)

SeNPs (b10a + b20a and c10a + c20a) were analyzed using an Agilent Cary 630 spectrometer (Palo Alto, CA, USA) in the range of 500 to 4,000 cm^{-1} with a resolution of 4 cm^{-1} and 64 scans in transmittance mode.

2.3.4. X-Ray Diffraction (XRD)

The analysis was performed on a STADI-P diffractometer (Stoe, Darmstadt, Germany) at room temperature, 40 kV, 20 mA, and using CuKα radiation (k = 1.54 A°). A Mythen 1 K detector (Dectris, Baden, Switzerland) was used to collect X-ray photons from a powder sample at a time interval of 2 h.

2.4. Tested strains

Standard American Type Culture Collection (ATCC) strains of *E. coli* ATCC 25922, *Pseudomonas aeruginosa* ATCC 27853, *S. aureus* ATCC 25923, *Streptococcus agalactiae* ATCC 13813, and Methicillin-resistant *S. aureus* (MRSA) BEC 9393 were used. The strains were stored in Brain Heart Infusion (BHI) broth (Difco®) containing 20% glycerol (Sigma-Aldrich®) at −80 °C.

2.5. Minimal inhibitory concentration (MIC) and minimal bactericidal concentration (MBC)

The broth microdilution assay was performed to obtain the MICs of the synthesized SeNPs against the strains mentioned above, according to the Clinical & Laboratory Standards Institute (CLSI) [32], with some modifications. The bacterial strains of *S. aureus*, MRSA, *E. coli*, and *P. aeruginosa* were grown on Mueller-Hinton agar (MHA) (Acumedia®), while *S. agalactiae* was grown on BHI agar and incubated for 24 h at 37 °C.

The microdilution assay was performed in a 96-well polyethylene microplate (Corning®), with SeNPs at eight concentrations, ranging from 1.531 to 196 μg/ml, diluted in Mueller-Hinton broth (MHB). Bacteria were added to each well at a final concentration of 5×10^5 colony forming units per ml (CFU/ml) and the microplate was incubated at 37 °C for 24 h. The MIC_{50} was performed by visual reading, and the minimum concentration was verified by visualizing the turbidity.

The tests were performed in triplicate, containing positive controls (only bacteria), sterility controls (only culture medium), extract controls (only extracts without nanoparticles), and sodium selenite controls (only sodium selenite in the same concentrations of the nanoparticles). Boldo + acerola and onion + acerola extracts without SeNPs were also performed.

The MBC was performed after the 24 h incubation by plating 10 μl of each well in MHA, followed by 18–24 h incubation at 37 °C for CFU counting. The MBC was determined at the concentration when bacterial death is ≥ 99.9% in the period of 24 h under treatment [33].

2.6. Time-kill assay

The test was done according to National Committee for Clinical Laboratory Standards (NCCLS) [33]. All strains were grown in MHA at 37 °C, for 18–24 h, except for *S. agalactiae*, which used BHI medium. A bacterial suspension was added to a microtube containing MHB at a final concentration of 5×10^5 CFU/ml for each strain. SeNPs were added to each microtube at the respective MICs, followed by incubation at 37 °C. Aliquots were taken at different incubation times (0, 1, 3, 5, 7, 9, 12, and 24 h) for dilution and plating in MHA to determine CFU/ml. A logarithmic survival curve was constructed as a function of the incubation and treatment times.

2.7. Cytotoxicity assay with human red blood cells

Hemolytic activity of SeNPs was performed according to Izumi et al. [34] with modifications. The blood was collected from a healthy human donor in heparinized tubes with the approval of the human ethics committee (CAAE47661115.0.0000.5231, No. 1.268.019 - UEL). The tubes were centrifuged at 2700×*g*, 4 °C for 5 min, the plasma was discarded, and the red blood cells were diluted in PBS (pH 7.4) at a concentration of 6% (v/v).

The test was performed at a 96-well plate, with SeNPs at final concentrations ranging from 1.531 to 196 μg/ml and red blood cells at 3%. The plate was incubated at 37 °C for 3 h, and the supernatant was read on a spectrophotometer (Biotek Synergy ™ HTX Multi-Mode Microplate Reader) at 550 nm. Triton X-100 (Sigma-Aldrich®) at 1% was used as a positive control, representing 100% hemolysis, and PBS was used as a negative control, representing 0% hemolysis.

2.8. Statistics

Data were analyzed using the software PAST (4.03) and GraphPad Prism 9. Analysis of variance (ANOVA) was carried out between the groups, and Tukey's post-test, with $p < 0.05$ statistically significant. Linear regression was performed to obtain CC_{50}. The results were presented as Mean ± standard deviation (SD).

3. Results

3.1. Synthesis

SeNPs biosynthesis was monitored for six days (Fig. 1), observing the solution coloring. The color change to red indicates Se^{+4} to Se^0 reduction [35]. This change occurred with great intensity on day three, and no change was observed between days 3–6, indicating the end of SeNPs biosynthesis. The acquired color can also reveal the morphology of the nanoparticles since red solutions tend to be monocyclic or amorphous, and dark and black solutions tend to have trigonal, linear, or rod shapes [36–38].

3.2. Electron microscopy (SEM) images

The synthesized SeNPs solutions b10a, b20a, c10a, and (Fig. 2a, b, c and d, respectively) were analyzed for their morphology and size by SEM. They all presented approximately spherical morphology, not visually showing changes in shapes among the different extracts and salt concentrations used.

The average diameter of the nanoparticles was measured with the software ImageJ, ranging from 245 (c20a) to 321 nm (b10a), as shown in Fig. 3.

3.3. Zeta potential and polydispersity index

The zeta potential value varied from −26 to −23 mV (Table 1). Values of ±0–10 mV, ± 10–20 mV, ± 20–30 mV, and ˃ ± 30 mV are, respectively, very unstable, little stable, stable and very stable [39]. All SeNPs had zeta potential between −20 and −30 mV, indicating stable nanoparticles in solution.

The polydispersity index (PDI) demonstrates the solution homogeneity. Its value ranges from 0 to 1, with 0 being an ideal solution in which all particles have the same size and 1 a highly polydispersed solution having particles with different sizes. Values below 0.5 are considered monodispersed, and values above 0.7 are considered highly polydispersed [40]. All samples analyzed had PDI below 0.5, ranging from 0.15 to 0.43 (Table 1), indicating a uniform size in solution, being stable and monodisperse.

3.4. Fourier-Transform Infrared Spectroscopy (FTIR)

Fig. 4c shows the spectra of b10a and b20a SeNPs. The bands at 3262 cm^{-1}, 2935 cm^{-1}, 1606 cm^{-1}, 1312 cm^{-1}, 1059 cm^{-1}, and 763 cm^{-1}

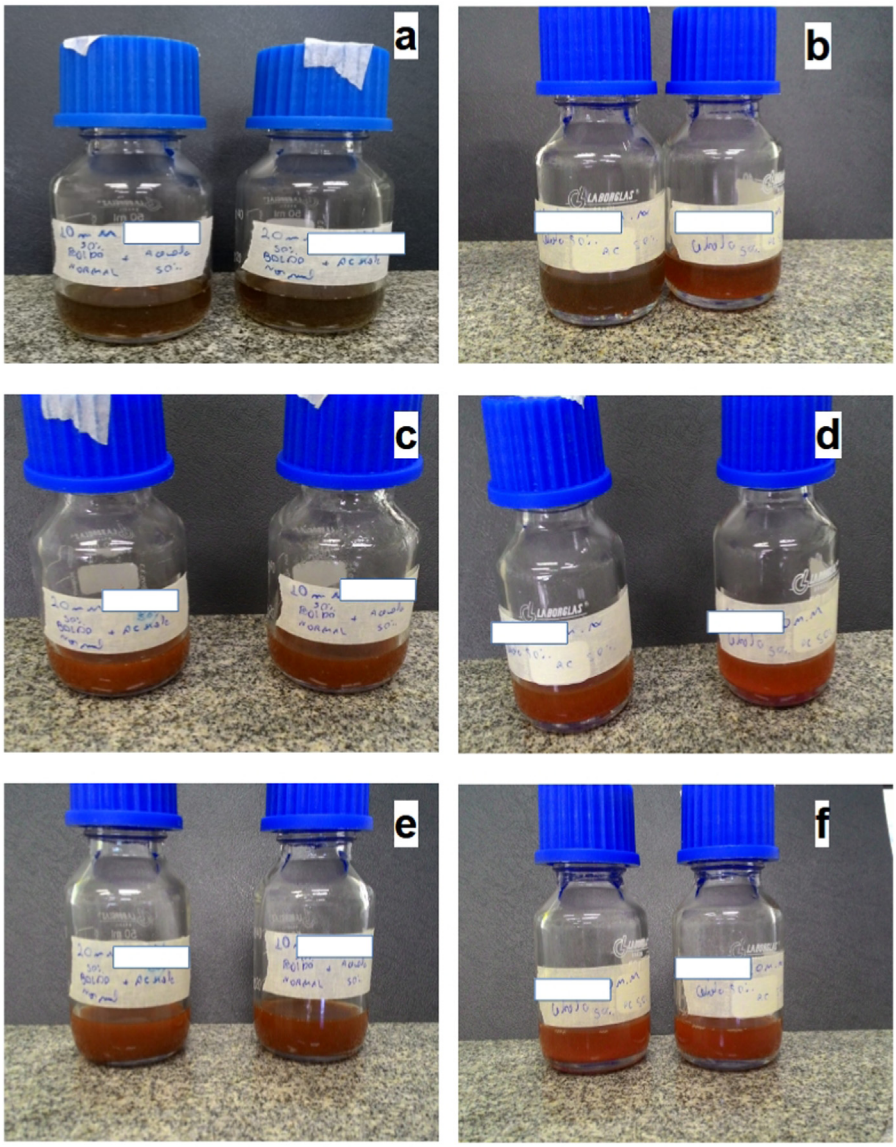

Fig. 1. Biosynthesis of SeNPs with extracts of onion + acerola (c10a and c20a) and boldo + acerola (b10a and b20a). (a) b10a and b20a on day 0. (b) c10a and c20a on day 0. (c) b10a and b20a on day 3. (d) c10a and c20a on day 3. (e) b10a and b20a on day 6. (f) c10a and c20a on day 6.

found Fig. 4c are associated respectively with the O–H, C–H, C═O, C═C, N–H, and C–O–C stretches, indicate the involvement of functional groups, mainly reducing agents such as ascorbic acid present in acerola, during the formation of SeNPs [41,42]. These bands indicate the presence of carboxylic acid, aromatic groups, phenolic compounds, and glycosidic bonds related to the cellulosic chain, indicating the formation of SeNPs associated with the bioactive provided by the molecules that make up the extracts of *M. emarginata* and *G. amygdalinum* used to synthesize b10a and b20a in the present work [42–44].

Fig. 4d illustrates the spectra of c10a and c20a SeNPs. The bands at 3281 cm^{-1}, 2923 cm^{-1}, 2846 cm^{-1}, 1611 cm^{-1}, 1031 cm^{-1}, and 781 cm^{-1} found in Fig. 4d) are associated with the O–H, CH_2, C–H, N–H, and C–O–C, indicating the involvement of functional groups during the formation of SeNPs [42,45]. The bands related to C–H, N–H, and C–O–C bending, respectively represented by the peaks at 2846 cm^{-1}, 1611 cm^{-1}, 1031 cm^{-1}, and 781 cm^{-1}, indicate the presence of polysaccharides such as cellulose, aromatic compounds, acidic groups such as carboxylic acid, phenolic compounds and lignin relating the formation of SeNPs associated with the bioactives provided by the molecules that make up the extracts of *M. emarginata* [43,45].

3.5. X-Ray Diffraction (XRD)

The crystal structure and the phase composition of SeNPs were determined using XRD technique, as shown in Fig. 4a and b. Through XRD it was possible to observe a crystal structure belonging to SeNPs b10a and b20a (Fig. 4a). The diffraction peaks at 2θ values of 14.46°, 32.39°, 40.25°, 46.45°, 47.95°, 49.63°, 52.81°, and 67.56°, respectively, corresponded to the revision plan (100), (101), (110), (102), (111), structure (201), (112) and (210), referring to trigonal structures of Se (t-Se) indicating the formation of crystalline SeNPs [46–48]. The amorphous structures, which do not have diffraction peaks, probably correspond to the formation of amorphous and monocyclic SeNPs or also called red Se(0) [48,49].

Fig. 4b demonstrates the XRD spectra belonging to the crystal structure of SeNPs c10a and c20a. The diffraction peaks at 2θ values of 14.29°, 32.51°, 40.25°, 46.45°, 47.98°, 49.70°, 52.79°, and 67.74° respectively corresponded to the plane of reflections (100), (101), (110), (102), (111), (201), (112) and (210), they correspond to t-Se structures, in addition to indicating a large amount of amorphous material that probably represents cyclic Se^0 [47,48].

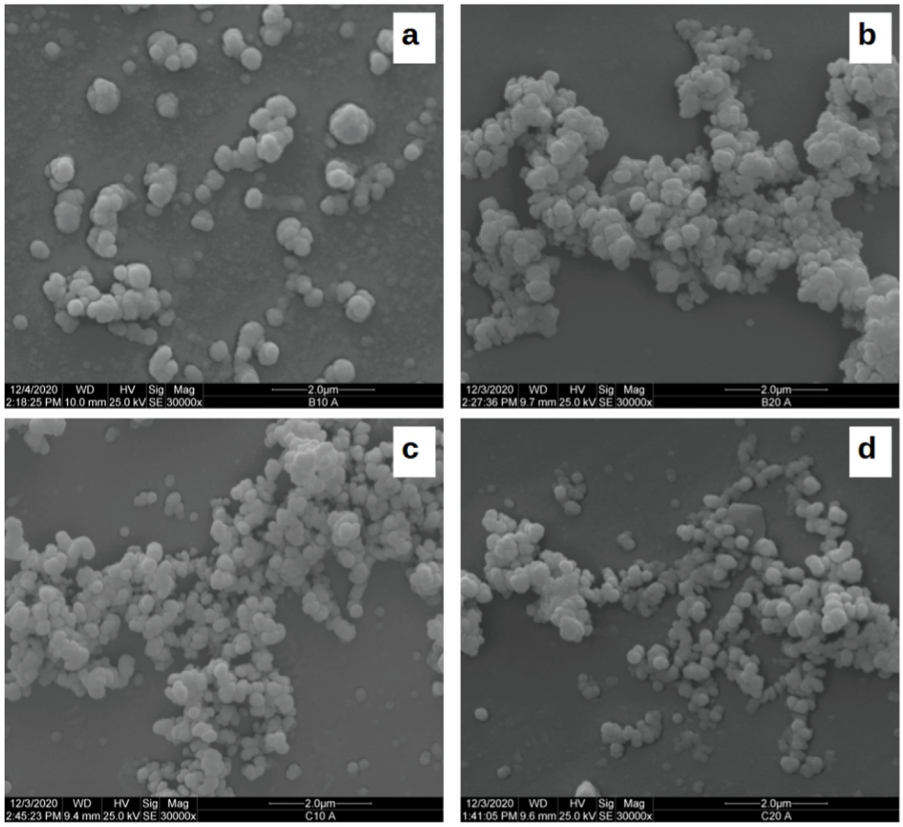

Fig. 2. SeNPs images made by scanning electron microscopy. (a) b10a (boldo + acerola extract with 10 mM sodium selenite). (b) b20a (boldo + acerola extract with 20 mM sodium selenite). (c) c10a (onion + acerola extract with 10 mM sodium selenite). (d) c20a (onion + acerola extract with 20 mM sodium selenite).

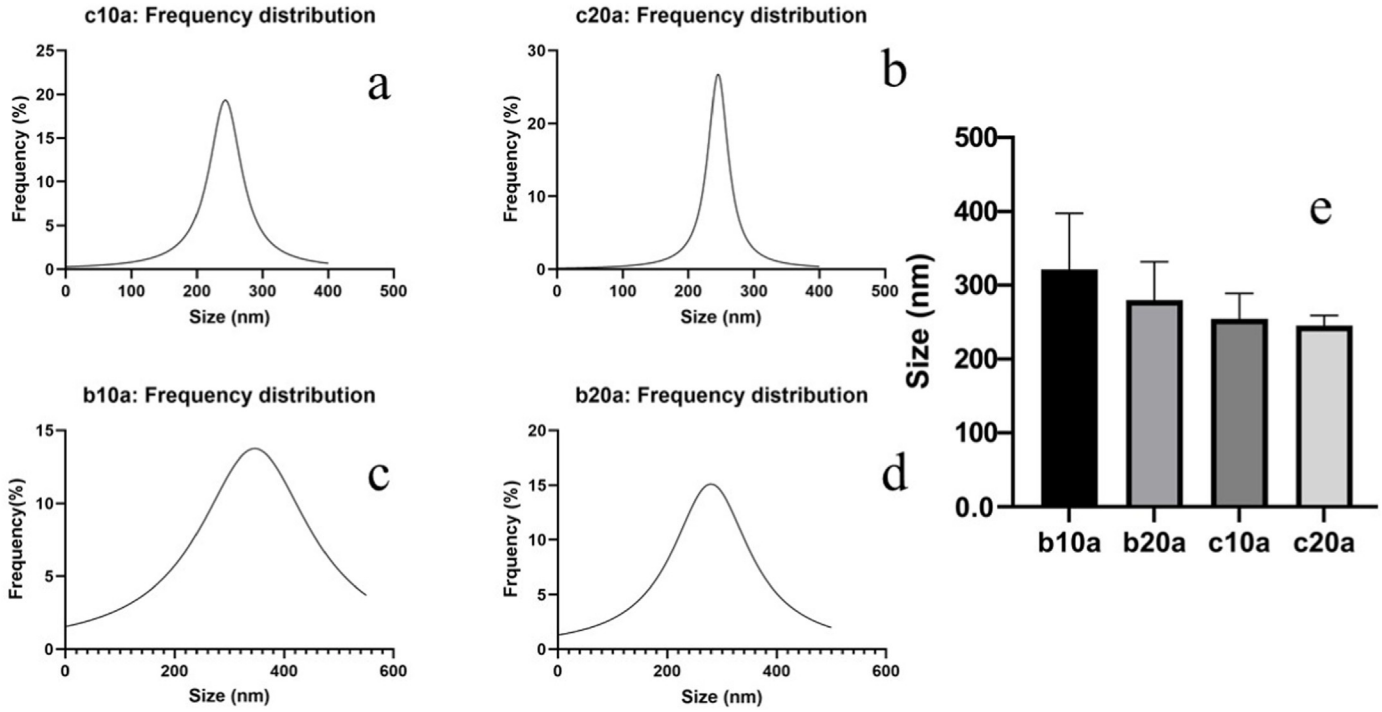

Fig. 3. (a),(b),(c),(d) histogram of the average size distribution of nanoparticles c10a, c20a, b10a and b20a, respectively. (e) Average size of SeNPs measured by ImageJ software from scanning electron microscopy images mean ± SD. b10a and b20a (10 and 20 mM sodium selenite, respectively, with boldo + acerola extract). c10a and c20a (10 and 20 mM sodium selenite, respectively, with onion + acerola extract).

Table 1
Polydispersity index (PDI) and zeta potential of SeNPs performed by DLS. b10a and b20a (10 and 20 mM sodium selenite, respectively, with boldo + acerola extract). c10a and c20a (10 and 20 mM sodium selenite, respectively, with onion + acerola extract). Mean ± SD.

Compounds	PDI	Zeta potential (mV)
b10a	0.27 ± 0.03	−23.46 ± 0.40
b20a	0.36 ± 0.15	−25.13 ± 0.55
c10a	0.42 ± 0.03	−23.93 ± 0.20
c20a	0.39 ± 0.01	−26.93 ± 0.32

3.6. Antibacterial activity

3.6.1. Minimal inhibitory concentration (MIC) and minimal bactericidal concentration (MBC)

Plant extracts without nanoparticles and sodium selenite tested against bacterial strains did not show antimicrobial activity at the concentrations used. *S. agalactiae* had the lowest MIC found in this study, 6.25 μg/ml for all tested SeNPs. *S. aureus* had MIC ranging between 24 and 49 μg/ml, and the *S. aureus* multiresistant strain, BEC 9393, had a MIC between 49 and 98 μg/ml. All Gram-positive strains tested were sensitive to SeNPs; however, there was no activity against the Gram-negative bacteria tested (Table 2). There was no difference between the MICs of the SeNPs synthesized with 10 and 20 mM sodium selenite

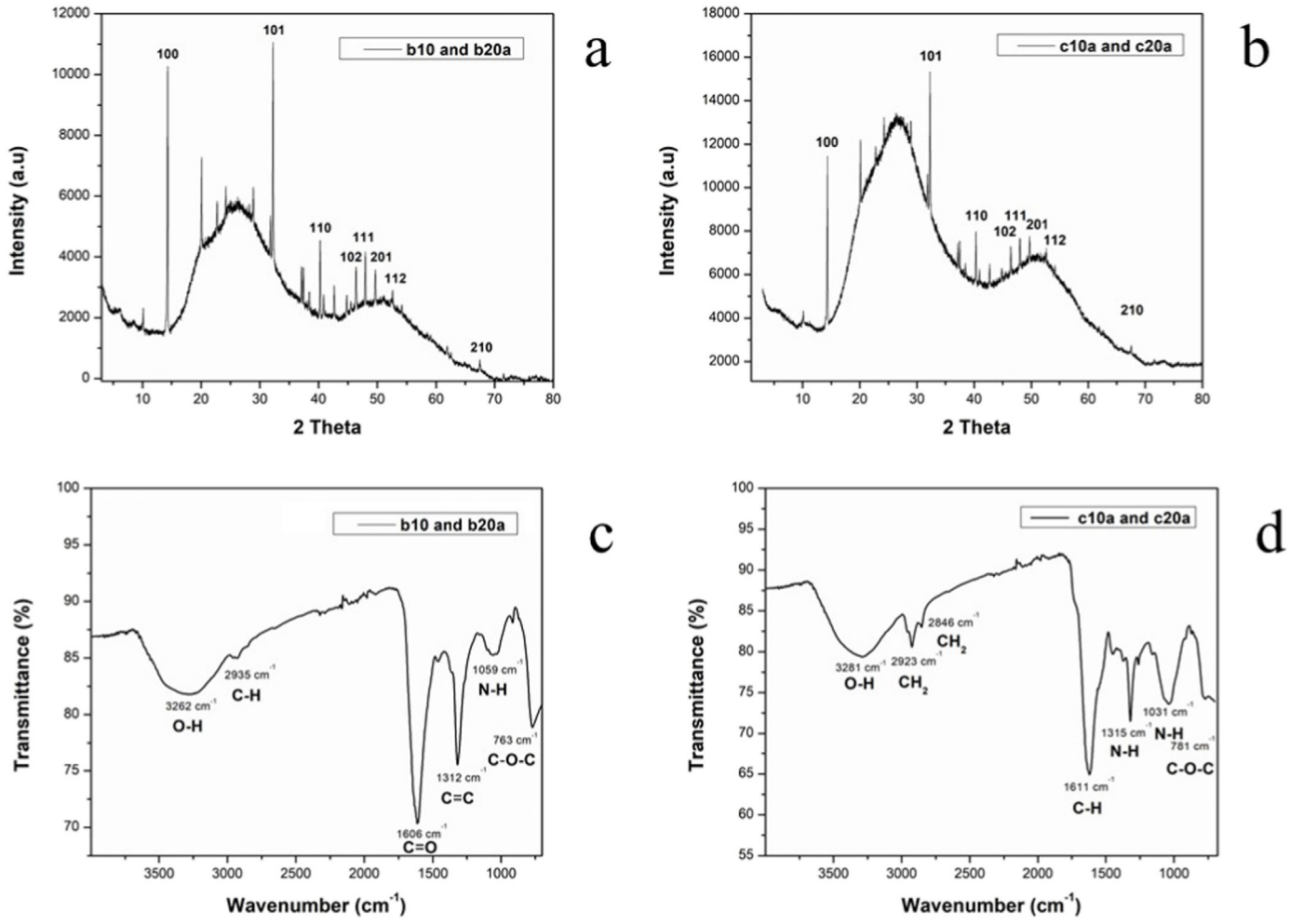

Fig. 4. (a) X-Ray Diffraction (XRD) of b10a and b20a. (b) XRD of c10a and c20a. (c) Fourier-Transform Infrared Spectroscopy (FTIR) of b10a and b20a. (d) FTIR of c10a and c20a. b10a and b20a (10 and 20 mM sodium selenite, respectively, with boldo + acerola extract). c10a and c20a (10 and 20 mM sodium selenite, respectively, with onion + acerola extract).

Table 2
Minimal inhibitory concentration and minimal bactericidal concentration of the SeNPs produced. c10a and c20a (biosynthesis with 10 and 20 mM sodium selenite, respectively, with onion extract + acerola). b10a and b20a (biosynthesis with 10 and 20 mM sodium selenite, respectively, with boldo + acerola extract).

	c10a (μg/ml)		c20a (μg/ml)		b10a (μg/ml)		b20a (μg/ml)	
TESTED BACTERIA	MIC	MBC	MIC	MBC	MIC	MBC	MIC	MBC
E. coli	>196	>196	>196	>196	>196	>196	>196	>196
P. aeruginosa	>196	>196	>196	>196	>196	>196	>196	>196
S. agalactiae	6.125	12.25	6.125	12.25	6.125	12.25	6.125	12.25
S. aureus	24.5	196	24,5	196	49	196	49	196
BEC 9393 (MRSA)	49	98	98	196	49	196	98	196

for the same bacteria, indicating that the salt concentration did not influence the antibacterial activity of the synthesized SeNPs.

The time-kill assay shows information about the kinetics and dynamics of the analyzed antimicrobials in contact with the strains. It is also possible to verify whether the compounds are bacteriostatic or bactericidal. Compounds are considered bactericidal when the bacterial concentration decreases ≥3 log10 of the initial inoculum concentration [50]. It is also possible to quantify bacterial death by time and antimicrobial concentration.

Regarding the *S. agalactiae* strain (Fig. 5a), all compounds, except b10a, showed a close action, but less than 3 log10, being classified as bacteriostatic. b10a also had bacteriostatic action; however, no decrease in bacterial counting was observed. It is worth mentioning that there was an increase in the number of bacteria for all SeNPs from 0 to 3 h, and after that period, the compounds started to show antibacterial action. This fact indicates the need for at least 3 h of treatment for antibacterial effect against *S. agalactiae*.

About *S. aureus* (Fig. 5b), none of the compounds showed a decrease in CFU, being considered bacteriostatic. In addition, its action ceased between 7 and 24 h, with less activity in 24 h. Concerning *S. aureus* BEC 9393 strain (Fig. 5c), only c20a showed a decrease of 3 log10 in bacterial concentration at 6 h, and c10a showed a reduction in the bacterial count of almost 3 log10 at 9 h. The other compounds presented a reduction in CFU at 3 h, but bacterial growth resumed after that. Resumption of bacterial growth was observed between 12 and 24 h in all tested SeNPs, revealing a decrease in antibacterial activity in this period.

3.7. Cytotoxicity assay with human red blood cells (RBC)

The extracts without nanoparticles were not hemolytic, and the SeNPs hemolysis is shown in Fig. 6. Through linear regression, it was possible to obtain the CC_{50} (minimal concentration that decreases 50% of the cell quantity) of the SeNPs, which were 1.6, 2.1, 1.5, and 1.67 mg/ml for c10a, c20a, b10a, and b20a, respectively.

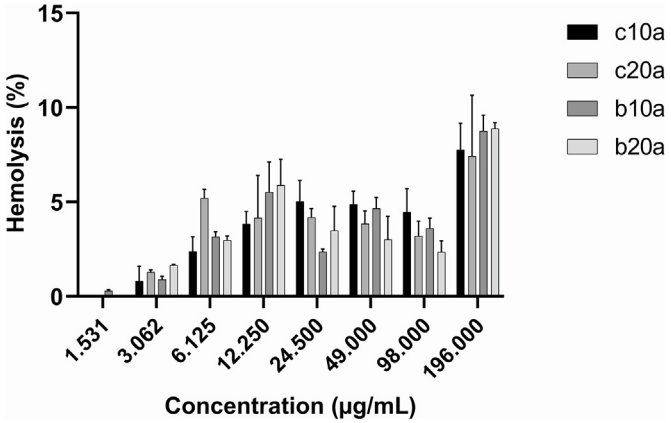

Fig. 6. Graph of the SeNPs, c10a and c20a hemolysis test (biosynthesis with 10 and 20 mM sodium selenite, respectively, with onion extract + acerola). b10a and b20a (biosynthesis with 10 and 20 mM sodium selenite, respectively, with boldo + acerola extract). Mean ± SD.

4. Discussion

To our knowledge to date, the present study is the first to synthesize SeNPs using a combination of two plant extracts, one of which is *G. amygdalinum* (boldo). SeNPs are commonly produced by chemical synthesis, where reagents such as sodium borohydride ($NaBH_4$), which is harmful and can react with water to form flammable gases, are commonly used [18,35]. The biosynthesis of SeNPs from plant extracts is

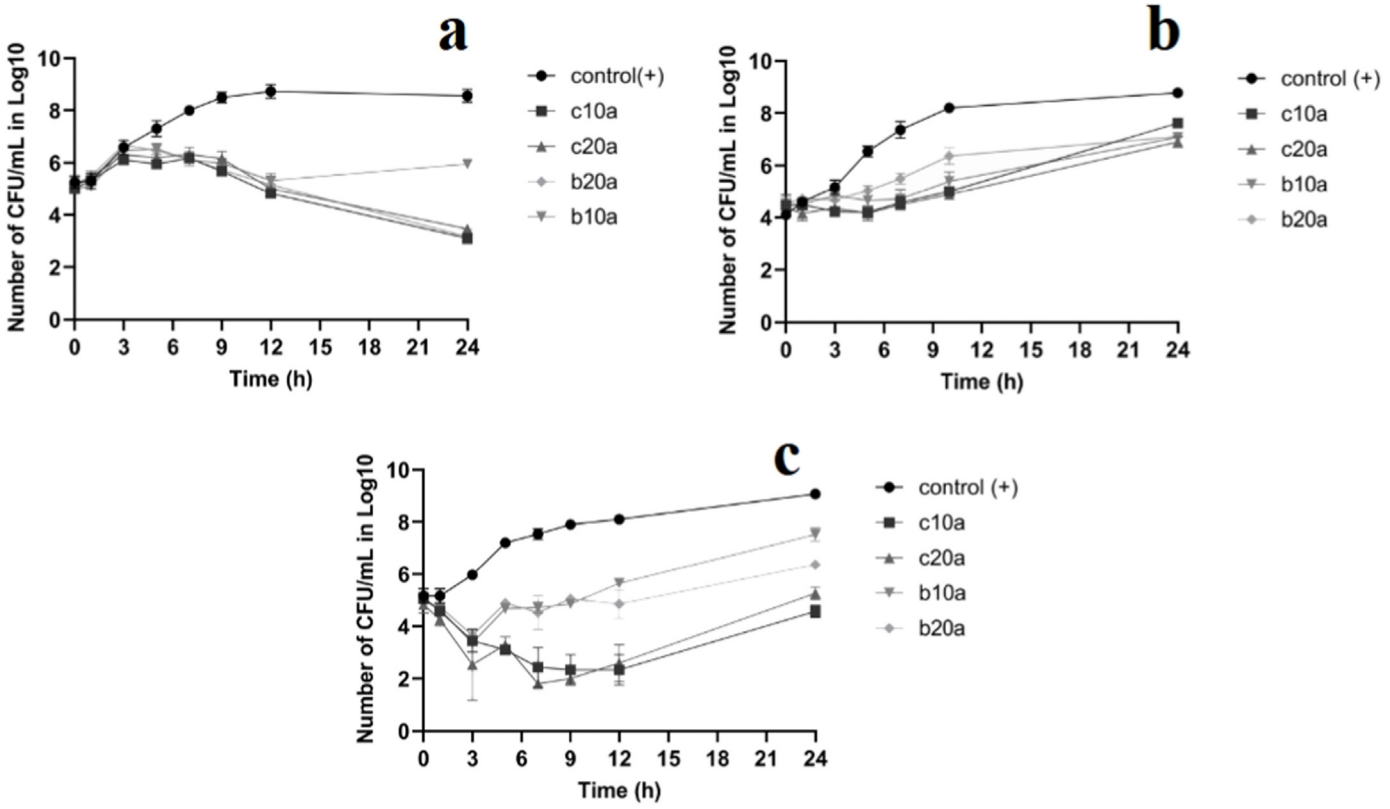

Fig. 5. (a), (b), and (c) Time-kill curves of *S. agalactiae* ATCC 13813, *S. aureus* ATCC 25923, methicillin-resistant *S. aureus* (MRSA) BEC 9393, respectively. c10a and c20a (biosynthesis with 10 and 20 mM sodium selenite, respectively, with onion + acerola extract). b10a and b20a (biosynthesis with 10 and 20 mM sodium selenite, respectively, with boldo + acerola extract). Mean ± SD.

less toxic, not generating toxic compounds to the environment.

The plants used in this study (boldo, onion, and acerola) are accessible, commonly found in markets and homes throughout Brazil, and have low cost compared to the chemical synthesis products. Onion and boldo have high amounts of quercetin, a flavonoid that has antimicrobial activity against some Gram-positive bacteria. The use of purified quercetin for SeNPs stabilization in chemical synthesis has already been performed, and antimicrobial efficacy against *S. aureus* was demonstrated [35].

Acerola has high amounts of ascorbic acid, a reducing agent used to synthesize several essential structures in the human body. Vahdati and Moghadam [51] performed SeNPs synthesis using ascorbic acid as a reducer and verified antibacterial action against *S. aureus*. As demonstrated, studies performed with some molecules found in the extracts used in the present study show efficiency in the SeNP synthesis and antimicrobial action. Therefore, the combination of plants for SeNPs synthesis is based on using extracts to increase the amount of reducing molecules and possibly stabilizing molecules.

The bacteria tested in this study have great medical significance. *S. aureus* is commonly found on skin microbiota; however, skin lesions can promote bacterial entry to the bloodstream, causing endocarditis, pneumonia, osteomyelitis, and other infections [52]. This pathogen is found in hospitals and the community, and some strains, such as MRSA, are resistant to antibiotics, making its control even more complex [53].

S. agalactiae causes neonatal infections and is the most common cause of sepsis in this group [54,55]. The infection occurs through transmission from the colonized mother to the newborn, and treatment consists of antibiotic administration to the mother, which can greatly affect the newborn's microbiota composition [54,56,57].

E. coli is typically found in the intestinal microbiota; however, pathogenic strains are the most significant cause of diseases in humans and the biggest responsible for urinary tract infections. Furthermore, *E. coli* resistant to several cephalosporins and fluoroquinolones, antibiotics commonly used in human medicine, have already been reported [58].

P. aeruginosa, a bacterium of great medical importance that inhabits soil, water, plants, and animals, can be resistant to multiple antimicrobial classes and cause infections, especially in immunocompromised patients [59].

SeNPs synthesized in the present work (c10a, c20a, b10a, and b20a) demonstrated antibacterial activity against some of the described strains, namely *S. aureus*, MRSA, and *S. agalactiae*, demonstrating a restricted antibacterial action for the Gram-positive tested.

The two Gram-negative bacteria tested, *E. coli* and *P. aeruginosa*, were not sensitive to nanoparticles at the evaluated concentrations. This result agrees with Nguyen et al. [2], who tested the antibacterial action of SeNPs in *S. aureus*, *E. coli*, and *Salmonella*, in which only *S. aureus* was sensitive to the treatment. The SeNPs produced had a −32 mV charge, which was slightly higher than the value found in the present study.

According to Arakha et al. [60], *E. coli* surface charge is more negative compared to *S. aureus* since Gram-negative bacteria have an outer membrane formed of lipopolysaccharide (LPS), which can promote this difference in charge [61]. Possibly, there are interactions between the negative charges found on the bacterial surface and the SeNPs, causing repulsion and hindering the nanoparticles' actions in Gram-negative.

However, some studies show activity against Gram-negative bacteria. Huang et al. [62] performed SeNPs synthesis using two types of coatings, resulting in one solution with negative zeta potential and the other with a positive one, both containing SeNPs in an average size of 46 nm. The two solutions were tested against *E. coli*, and nanoparticles with positive charges showed better antibacterial action. The interaction between nanoparticles and *E. coli* was analyzed by SEM, revealing that nanoparticles with negative charge moved away from cells (equal charges) while the positive ones clustered with cells (opposite charges).

Khiralla and El-Deeb [30] also reported SeNPs action against *E. coli* and *Salmonella*. The synthesis was performed using *B. licheniformis* supernatant, and the average SeNPs size was 30 nm. Nevertheless, no data about zeta potential were presented, and the antibacterial tests of the *B. licheniformis* supernatant were not reported. Considering this fact, it is not possible to relate the antibacterial activity exclusively to the surface charge or the nanoparticles themselves since the presence of bacteriocins in the supernatant, which exerts the antibacterial action, cannot be discarded.

Zhang et al. [63] produced SeNPs with *Providencia* sp., obtaining nanoparticles with an average size of 120 nm and −25 mV of zeta potential. These SeNPs were more effective against *E. coli* and *P. aeruginosa* than *S. aureus*. It is interesting to note that the nanoparticles were half the size but similar to the current study. However, the results about the antibacterial action for Gram-positive and Gram-negative were the opposite.

The cited studies demonstrated the SeNPs action on Gram-negative bacteria, in which nanoparticle diameters obtained were smaller than those presented in the current study. This difference may indicate that the size and type of coating molecule play an important role in the antibacterial activity of nanoparticles. Regardless, the SeNPs produced vary according to the synthesis parameters, and nuances related to its antibacterial action in Gram-positive and Gram-negative bacteria are still obscure; however, there are some hypotheses for their antimicrobial activity. Huang et al. [64] found reactive oxygen species (ROS) production, ATP depletion, and membrane polarity change in *S. aureus* after treatment with SeNPs. ROS can damage the bacteria's DNA, membrane, and proteins, inhibiting its metabolism and leading to death.

SeNPs cytotoxicity in red blood cells can be related to numerous factors, such as size, type of coating, and stability in solution. Luesakul et al. [65], tested two sizes of SeNPs (198 and 322 nm) and observed that smaller nanoparticles had a greater cytotoxic effect. This fact occurs due to the increased contact surface and the ease of interiorization of smaller nanoparticles [15].

The cytotoxic effect of SeNPs on tumor cells has already been described [66]. Nguyen et al. [2] reported a reduction of up to 30% in the viability of Caco-2 cells tested with SeNPs. Luesakul et al. [65] observed the cytotoxic effect on breast cancer cells (BT474) and low cytotoxicity against normal lung cells (WI38). Generally, many studies indicate greater cytotoxic effects in tumor cell lines than normal cells [15,67].

Chen et al. [68] developed a methodology for the synthesis of SeNPs coated with polysaccharides. The nanoparticles produced showed increased cytotoxicity against tumoral cell lineages, which, according to the study, is due to DNA fragmentation and chromatin condensation, leading to cell apoptosis. Another study carried out with SeNPs coated in pectin demonstrated low toxicity in non-tumoral (RWPE-1) and tumoral cells (HeLa), which, according to the author, occurred due to the decrease in toxicity promoted by the pectin coat [69].

A study evaluating the cytotoxic effect of SeNPs synthesized with *Allium sativum* (garlic) showed a CC_{50} of 31 μg/ml on Vero cells, in which the nanoparticles had an average size of 70 nm [70].

The studies mentioned above indicate that several characteristics influence SeNPs' activity in preventing growth or promoting cell death. The cytotoxic tests performed on erythrocytes in the present study showed high CC_{50} and low cytotoxicity. Nevertheless, few studies reported SeNPs toxicity against red blood cells but compared to nucleated cells, the cytotoxicity in red blood cells was probably lower. These differences are probably related to the fact that erythrocytes are anucleate cells and, therefore, some possible cytotoxic mechanisms do not apply to them.

Metal and metal oxides nanoparticles have many applications with different strategies and aims, such as magnesium oxide nanoparticles for anti-arthritic and anti-cancer [71], iron oxide nanoparticles with electro-optical properties, biogenic silver nanoparticles as antibacterial, some nanomaterials to combat the Severe Acute Respiratory Syndrome Coronavirus-2 (SARS-CoV-2) pandemic, and ore@shell nanomaterials in the biosensing field [72–74].

The nanoparticles synthesized in this study showed desirable antibacterial activity against some bacterial strains, in addition to low

cytotoxicity in red blood cells, making SeNPs applicable in various products with antibacterial purposes. Furthermore, selenium is an essential micronutrient, with a required consumption of 300 μg/day, and a component of some proteins, such as glutathione peroxidases (GSH-Px), thioredoxin reductases (TRXR), and tetraiodothyronine deiodase (DIO) [18,75].

SeNPs absorption from products with antibacterial purposes, such as ointments or gels, will possibly not be harmful since selenium plays a role in the body's homeostasis. In this context, SeNPs show advantages over other products such as silver or gold nanoparticles since these metals do not participate in any biological process to maintain homeostasis and, therefore, are not useful for their absorption.

5. Conclusion

The biosynthesis of SeNPs (c10a, c20a, b10a, and b20a) was successfully performed, as indicated by SEM, DLS, FTIR, and XDR, demonstrating stable nanoparticles with chemical bonds corresponding to the extracts used. SeNPs demonstrated bacteriostatic and bactericidal action, which varied according to the exposure time and the tested bacteria. Antimicrobial activity against Gram-positive bacteria was relevant, but no activity against Gram-negative strains was observed, indicating a restriction in the spectrum of activity. Regarding hemolysis, the CC_{50} was low, indicating low cytotoxicity. Considering the fact that bacterial resistance is an increasing challenge for public health, compounds such as the SeNPs biosynthesized in the present study may become alternatives to antimicrobial control. Therefore, due to their antibacterial, antioxidant, and anti-inflammatory action, SeNPs can be added to lotions, ointments, and gels to treat wounds and burns. They can be used as growth promoters in poultry and can also be associated with probiotics. SeNPs can also be used in formulations of specific antimicrobial products for Gram-positive bacteria and soil supplementation in agriculture. There are several possibilities for the use of nanoparticles synthesized in the present work. The next step will be to refine the synthesis of SeNPs and test their applicability in the mentioned areas and products.

Declaration of competing interest

The authors declare no conflict of interest.

Acknowledgements

The authors are grateful to the Laboratory for Electron Microscopy – LMEM/university of Londrina for help with the electron microscopy experiments. Thanks also to the staff of the Federal University of ABC (Santo André – São Paulo, Brasil), especially the master Joana Pierreti for the DLS analyses.

References

[1] I. Mack, J. Bielicki, What can we do about antimicrobial resistance? Pediatr. Infect. Dis. J. 38 (2019) S33–S38, https://doi.org/10.1097/inf.0000000000002321.
[2] T.H. Nguyen, B. Vardhanabhuti, M. Lin, A. Mustapha, Antibacterial properties of selenium nanoparticles and their toxicity to Caco-2 cells, Food Control 77 (2017) 17–24, https://doi.org/10.1016/j.foodcont.2017.01.018.
[3] S. Scandorieiro, L.C.D. Camargo, C.A.C. Lancheros, S.F. Yamada-Ogatta, C.V. Nakamura, A.G.D. Oliveira, C.G.T.J. Andrade, N. Duran, G. Nakazato, R.K.T. Kobayashi, Synergistic and additive effect of oregano essential oil and biological silver nanoparticles against multidrug-resistant bacterial strains, Front. Microbiol. 7 (2016) 760, https://doi.org/10.3389/fmicb.2016.00760.
[4] S. Shamaila, N. Zafar, S. Riaz, R. Sharif, J. Nazir, S. Naseem, Gold nanoparticles: an efficient antimicrobial agent against enteric bacterial human pathogen, Nanomaterials 6 (2016) 71, https://doi.org/10.3390/nano6040071.
[5] L. Xiao, Y. Wang, Y. Yu, G. Fu, Y. Liu, Z. Sun, et al., Enhanced selective recovery of selenium from anode slime using MnO2 in dilute h2so4 solution as oxidant, J. Clean. Prod. 209 (2019) 494–504, https://doi.org/10.1016/j.jclepro.2018.10.144.
[6] H. Yu, Z. Qi, J. Zhang, Z. Wang, R. Sun, Y. Chang, et al., Tailoring non-fullerene acceptors using selenium-incorporated heterocycles for organic solar cells with over 16% efficiency, J. Mater. Chem. 8 (2020) 23756–23765, https://doi.org/10.1039/d0ta06658c.
[7] D. Radomska, R. Czarnomysy, D. Radomski, A. Bielawska, K. Bielawski, Selenium as a bioactive micronutrient in the human diet and its cancer chemopreventive activity, Nutrients 13 (2021) 1649, https://doi.org/10.3390/nu13051649.
[8] V. Nayak, K.R.B. Singh, A.K. Singh, R.P. Singh, Potentialities of selenium nanoparticles in biomedical science, New J. Chem. 45 (2021) 2849–2878, https://doi.org/10.1039/d0nj05884j.
[9] T. Filippini, S. Cilloni, M. Malavolti, F. Violi, C. Malagoli, M. Tesauro, et al., Dietary intake of cadmium, chromium, copper, manganese, selenium and zinc in a Northern Italy community, J. Trace Elem. Med. Biol. 50 (2018) 508–517, https://doi.org/10.1016/j.jtemb.2018.03.001.
[10] A. Abdel Moneim, S. Al-Quraishy, M.A. Dkhil, Anti-hyperglycemic activity of selenium nanoparticles in streptozotocin-induced diabetic rats, Int. J. Nanomed. (2015) 6741, https://doi.org/10.2147/ijn.s91377.
[11] I. Galan-Chilet, M. Grau-Perez, G. De Marco, E. Guallar, J.C. Martin-Escudero, A. Dominguez-Lucas, et al., A gene-environment interaction analysis of plasma selenium with prevalent and incident diabetes: The Hortega Study, Redox Biol. 12 (2017) 798–805, https://doi.org/10.1016/j.redox.2017.04.022.
[12] T. Chen, Y.-S. Wong, W. Zheng, Y. Bai, L. Huang, Selenium nanoparticles fabricated in Undaria pinnatifida polysaccharide solutions induce mitochondria-mediated apoptosis in A375 human melanoma cells, Colloids Surf. B Biointerfaces 67 (2008) 26–31, https://doi.org/10.1016/j.colsurfb.2008.07.010.
[13] J. Jeevanandam, A. Barhoum, Y.S. Chan, A. Dufresne, M.K. Danquah, Review on nanoparticles and nanostructured materials: History, sources, toxicity and regulations, Beilstein J. Nanotechnol. 9 (2018) 1050–1074, https://doi.org/10.3762/bjnano.9.98.
[14] M. Ikram, B. Javed, N.I. Raja, Z.-U.-R. Mashwani, Biomedical potential of plant-based selenium nanoparticles: a comprehensive review on therapeutic and mechanistic aspects, Int. J. Nanomed. 16 (2021) 249–268, https://doi.org/10.2147/ijn.s295053.
[15] S. Chaudhary, A. Umar, S. Mehta, Selenium nanomaterials: an overview of recent developments in synthesis, properties and potential applications, Prog. Mater. Sci. 83 (2016) 270–329, https://doi.org/10.1016/j.pmatsci.2016.07.001.
[16] S. Shoeibi, P. Mozdziak, A. Golkar-Narenji, Biogenesis of selenium nanoparticles using green chemistry, Top. Curr. Chem. 375 (2017) 88, https://doi.org/10.1007/s41061-017-0176-x.
[17] B. Zare, S. Babaie, N. Setayesh, A.R. Shahverdi, Isolation and characterization of a fungus for extracellular synthesis of small selenium nanoparticles, Nanomed. J 1 (2013) 13–19, https://doi.org/10.7508/NMJ.2013.01.002.
[18] B. Hosnedlova, M. Kepinska, S. Skalickova, C. Fernandez, B. Ruttkay-Nedecky, Q. Peng, et al., Nano-selenium and its nanomedicine applications: a critical review, Int. J. Nanomed. 13 (2018) 2107–2128, https://doi.org/10.2147/ijn.s157541.
[19] R.S. Oremland, M.J. Herbel, J.S. Blum, S. Langley, T.J. Beveridge, P.M. Ajayan, T. Sutto, A.V. Ellis, S. Curran, Structural and spectral features of selenium nanospheres produced by Se-respiring bacteria, Appl. Environ. Microbiol. 70 (2004) 52–60, https://doi.org/10.1128/AEM.70.1.52-60.2004.
[20] G.T. Galo, A.C. Lima, K.M. Machado, L.B. Vieira, V.C. Martins, N.L. Ferreira, et al., Estudo da Extração da quercetina a partir da Cebola Roxa (allium ceppa L.) e seu Uso Como Conservante Alimentar Natural, J. Eng. Exact Sci. 4 (2018), 0153–0162, https://doi.org/10.18540/jcecvl4iss1pp0153-0162.
[21] F. Wu, Y. Chen, G. Li, D. Zhu, L. Wang, J. Wang, Zinc oxide nanoparticles synthesized from allium cepa prevents UVB radiation mediated inflammation in human epidermal keratinocytes (HaCaT cells), Artificial Cells, Nanomedicine, Biotechnol. 47 (2019) 3548–3558, https://doi.org/10.1080/21691401.2019.1642905.
[22] E.Z. Gomaa, Antimicrobial, antioxidant and antitumor activities of silver nanoparticles synthesized by allium cepa extract: a green approach, J. Genetic Eng. Biotechnol. 15 (2017) 49–57, https://doi.org/10.1016/j.jgeb.2016.12.002.
[23] D. Jini, S. Sharmila, Green synthesis of silver nanoparticles from allium cepa and its in vitro antidiabetic activity, Mater. Today Proc. 22 (2020) 432–438, https://doi.org/10.1016/j.matpr.2019.07.672.
[24] C.B. Lopes, C.A. da Camara, M.M. de Moraes, Composition of essential oils from the leaves, stems, and flowers of Vernonia Condensata of Pernambuco, Brazil, Chem. Nat. Compd. 55 (2019) 756–758, https://doi.org/10.1007/s10600-019-02802-8.
[25] B.G. Brasileiro, V.R. Pizziolo, D.S. Raslan, C.M. Jamal, D. Silveira, Antimicrobial and cytotoxic activities screening of some Brazilian medicinal plants used in governador valadares district, Rev. Bras. Ciencias Farm. 42 (2006) 195–202, https://doi.org/10.1590/s1516-93322006000200004.
[26] R.L. Fabri, M.S. Nogueira, L.B. Dutra, M.L.M. Bouzada, E. Scio, Potential Antioxidante e antimicrobiano de Espécies da família asteraceae, Rev. Bras. Plantas Med. 13 (2011) 183–189, https://doi.org/10.1590/s1516-05722011000200009.
[27] J.M. Alvarez-Suarez, F. Giampieri, M. Gasparrini, L. Mazzoni, C. Santos-Buelga, A.M. González-Paramás, et al., The protective effect of acerola (malpighia emarginata) against oxidative damage in human dermal fibroblasts through the improvement of antioxidant enzyme activity and mitochondrial functionality, Food Funct. 8 (2017) 3250–3258, https://doi.org/10.1039/c7fo00859g.
[28] D.D. Leffa, G.T. Rezin, F. Daumann, L.M. Longaretti, A.L. Dajori, L.M. Gomes, et al., Effects of acerola (Malpighia emarginata DC.) juice intake on brain energy metabolism of mice fed a cafeteria diet, Mol. Neurobiol. 54 (2016) 954–963, https://doi.org/10.1007/s12035-016-9691-y.
[29] W.W. Andualem, F.K. Sabir, E.T. Mohammed, H.H. Belay, B.A. Gonfa, Synthesis of copper oxide nanoparticles using plant leaf extract of Catha edulis and its antibacterial activity, J. Nanotechnol. 2020 (2020) 1–10, https://doi.org/10.1155/2020/2932434.
[30] G.M. Khiralla, B.A. El-Deeb, Antimicrobial and antibiofilm effects of selenium nanoparticles on some foodborne pathogens, LWT 63 (2015) 1001–1007, https://doi.org/10.1016/j.lwt.2015.03.086.

[31] X. Huang, X. Chen, Q. Chen, Q. Yu, D. Sun, J. Liu, Investigation of functional selenium nanoparticles as potent antimicrobial agents against superbugs, Acta Biomater. 30 (2016) 397–407, https://doi.org/10.1016/j.actbio.2015.10.041.
[32] CLSI (THE CLINICAL & LABORATORY STANDARDS INSTITUTE), Methods for Dilution Antimicrobial Susceptibility Tests of Bacteria that Grow Aerobically, Document M07, A10—tenth ed., CLSI, Wayne, PA, USA, 2015.
[33] NCCLS, Methods for Determining Bactericidal Activity of Antimicrobial Agents, 1999.
[34] E. Izumi, T. Ueda-Nakamura, V.F. Veiga, A.C. Pinto, C.V. Nakamura, Terpenes from copaifera demonstrated in vitro antiparasitic and synergic activity, J. Med. Chem. 55 (2012) 2994–3001, https://doi.org/10.1021/jm201451h.
[35] T. Wang, L. Yang, B. Zhang, J. Liu, Extracellular biosynthesis and transformation of selenium nanoparticles and application in H2O2 biosensor, Colloids Surf., B 80 (2010) 94–102, https://doi.org/10.1016/j.colsurfb.2010.05.041.
[36] X.B. Cao, Y. Xie, S.Y. Zhang, F.Q. Li, Ultra-thin trigonal selenium nanoribbons developed from series-wound beads, Adv. Mater. 16 (2004) 649–653, https://doi.org/10.1002/adma.200306317.
[37] C.T. Ho, J.W. Kim, W.B. Kim, K. Song, R.A. Kanaly, M.J. Sadowsky, et al., Shewanella-mediated synthesis of selenium nanowires and nanoribbons, J. Mater. Chem. 20 (2010) 5899, https://doi.org/10.1039/b923252d.
[38] H. Dong, A. Quintilla, M. Cemernjak, R. Popescu, D. Gerthsen, E. Ahlswede, et al., Colloidally stable selenium@copper selenide core@shell nanoparticles as selenium source for manufacturing of copper–indium–selenide solar cells, J. Colloid Interface Sci. 415 (2014) 103–110, https://doi.org/10.1016/j.jcis.2013.10.001.
[39] S. Bhattacharjee, DLS and zeta potential – what they are and what they are not? J. Contr. Release 235 (2016) 337–351, https://doi.org/10.1016/j.jconrel.2016.06.017.
[40] M. Danaei, M. Dehghankhold, S. Ataei, F.H. Davarani, R. Javanmard, A. Dokhani, et al., Impact of particle size and polydispersity index on the clinical applications of lipidic nanocarrier systems, Pharmaceutics 10 (2018) 57, https://doi.org/10.3390/pharmaceutics10020057.
[41] G.B. Alvi, M.S. Iqbal, M.M. Ghaith, A. Haseeb, B. Ahmed, M.I. Qadir, Biogenic selenium nanoparticles (senps) from citrus fruit have anti-bacterial activities, Sci. Rep. 11 (2021), https://doi.org/10.1038/s41598-021-84099-8.
[42] A.C.P. Silva, A.O. Jorgetto, M.H.P. Wondracek, R.M. Galera, J.F. Schneider, M.J. Saeki, et al., Properties, characteristics and application of grinded Malpighia emarginata seeds in the removal of toxic metals from water, Groundwater Sustain. Develop. 6 (2018) 50–56, https://doi.org/10.1016/j.gsd.2017.10.006.
[43] J.D. Silva, D.E. Santos, A.K. Abud, A.M. Oliveira, Characterization of acerola (malpighia emarginata) industrial waste as raw material for thermochemical processes, Waste Manag. 107 (2020) 143–149, https://doi.org/10.1016/j.wasman.2020.03.037.
[44] P. Ragavan, A. Ananth, M.R. Rajan, Impact of selenium nanoparticles on growth, biochemical characteristics and yield of cluster Bean Cyamopsis tetragonoloba, Int. J. Environ. Agriculture Biotechnol. 2 (2017) 2917–2926, https://doi.org/10.22161/ijeab/2.6.19.
[45] N. Carvalho Gualberto, C. Santos de Oliveira, J. Pedreira Nogueira, M. Silva de Jesus, H. Caroline Santos Araujo, M. Rajan, et al., Bioactive compounds and antioxidant activities in the agro-industrial residues of Acerola (Malpighia emarginata L.), guava (psidium guajava L.), GENIPAP (genipa americana L.) and Umbu (spondias tuberosa L.) fruits assisted by ultrasonic or shaker extraction, Food Res. Int. 147 (2021) 110538, https://doi.org/10.1016/j.foodres.2021.110538.
[46] F. Jiang, W. Cai, G. Tan, Facile synthesis and optical properties of small selenium nanocrystals and nanorods, Nanoscale Res. Lett. 12 (2017), https://doi.org/10.1186/s11671-017-2165-y.
[47] G.D.R. Nogueira, C.R. Duarte, M.A.S. Barrozo, Hydrothermal carbonization of Acerola (Malphigia emarginata D.C.) wastes and its application as an adsorbent, Waste Manag. 95 (2019) 466–475, https://doi.org/10.1016/j.wasman.2019.06.039.
[48] K.S. Prasad, K. Selvaraj, Biogenic synthesis of selenium nanoparticles and their effect on as(iii)-induced toxicity on human lymphocytes, Biol. Trace Elem. Res. 157 (2014) 275–283, https://doi.org/10.1007/s12011-014-9891-0.
[49] M.A. Ruiz Fresneda, J. Delgado Martín, J. Gómez Bolívar, M.V. Fernández Cantos, G. Bosch-Estévez, M.F. Martínez Moreno, et al., Green synthesis and biotransformation of amorphous se nanospheres to trigonal 1d se nanostructures: impact on se mobility within the concept of radioactive waste disposal, Environ. Sci.: Nano 5 (2018) 2103–2116, https://doi.org/10.1039/c8en00221e.
[50] C. Bozkurt-Guzel, G. Inci, O. Oyardi, P.B. Savage, Synergistic activity of ceragenins against carbapenem-resistant acinetobacter baumannii strains in both checkerboard and dynamic time-kill assays, Curr. Microbiol. 77 (2020) 1419–1428, https://doi.org/10.1007/s00284-020-01949-w.
[51] M. Vahdati, T.T. Moghadam, Synthesis and characterization of selenium nanoparticles-lysozyme nanohybrid system with synergistic antibacterial properties, Sci. Rep. 10 (2020), https://doi.org/10.1038/s41598-019-57333-7.
[52] S.Y.C. Tong, J.S. Davis, E. Eichenberger, T.L. Holland, V.G. Fowler, Staphylococcus aureus infections: epidemiology, pathophysiology, clinical manifestations, and management, Clin. Microbiol. Rev. 28 (2015) 603–661, https://doi.org/10.1128/cmr.00134-14.
[53] A.S. Lee, H.D. Lencastre, J. Garau, J. Kluytmans, S. Malhotra-Kumar, A. Peschel, et al., Methicillin-resistant Staphylococcus aureus, Nat. Rev. Dis. Prim. (2018) 4, https://doi.org/10.1038/nrdp.2018.33.
[54] A.F. Dagnew, M.C. Cunnington, Q. Dube, M.S. Edwards, N. French, R.S. Heyderman, et al., Variation in reported neonatal group B streptococcal disease incidence in developing countries, Clin. Infect. Dis. 55 (2012) 91–102, https://doi.org/10.1093/cid/cis395.
[55] A. Schuchat, Group B streptococcus, Lancet 353 (1999) 51–56, https://doi.org/10.1016/s0140-6736(98)07128-1.
[56] I. Aloisio, A. Quagliariello, S.D. Fanti, D. Luiselli, C.D. Filippo, D. Albanese, et al., Evaluation of the effects of intrapartum antibiotic prophylaxis on newborn intestinal microbiota using a sequencing approach targeted to multi hypervariable 16S rDNA regions, Appl. Microbiol. Biotechnol. 100 (2016) 5537–5546, https://doi.org/10.1007/s00253-016-7410-2.
[57] N.J. Russell, A.C. Seale, M. O'Driscoll, C. O'Sullivan, F. Bianchi-Jassir, J. Gonzalez-Guarin, et al., Maternal colonization with group B Streptococcus and serotype distribution worldwide: systematic review and meta-analyses, Clin. Infect. Dis. 65 (2017), https://doi.org/10.1093/cid/cix658.
[58] World Health Organization, Antimicrobial Resistance: Global Report on Surveillance, World Health Organization, 2014.
[59] European Centre for Disease Prevention and Control, Surveillance of Antimicrobial Resistance in Europe–Annual Report of the European Antimicrobial Resistance Surveillance Network (EARS-Net) 2017, S. ECDC, 2018.
[60] M. Arakha, M. Saleem, B.C. Mallick, S. Jha, The effects of interfacial potential on antimicrobial propensity of ZnO nanoparticle, Sci. Rec. 5 (2015), https://doi.org/10.1038/srep09578.
[61] S. Halder, K.K. Yadav, R. Sarkar, S. Mukherjee, P. Saha, S. Haldar, et al., Alteration of Zeta potential and membrane permeability in bacteria: a study with cationic agents, SpringerPlus 4 (2015), https://doi.org/10.1186/s40064-015-1476-7.
[62] T. Huang, S. Kumari, H. Herold, H. Bargel, T.B. Aigner, D.E. Heath, et al., Enhanced antibacterial activity of Se nanoparticles upon coating with recombinant spider silk protein eADF4(κ16), Int. J. Nanomed. 15 (2020) 4275–4288, https://doi.org/10.2147/ijn.s255833.
[63] H. Zhang, Z. Li, C. Dai, P. Wang, S. Fan, B. Yu, et al., Antibacterial properties and mechanism of selenium nanoparticles synthesized by Providencia sp. DCX, Environ. Res. 194 (2021) 110630, https://doi.org/10.1016/j.envres.2020.110630.
[64] T. Huang, J.A. Holden, D.E. Heath, N.M. Obrien-Simpson, A.J. Oconnor, Engineering highly effective antimicrobial selenium nanoparticles through control of particle size, Nanoscale 11 (2019) 14937–14951, https://doi.org/10.1039/c9nr04424h.
[65] U. Luesakul, S. Komenek, S. Puthong, N. Muangsin, Shape-controlled synthesis of cubic-like selenium nanoparticles via the self-assembly method, Carbohydr, Polymer 153 (2016) 435–444, https://doi.org/10.1016/j.carbpol.2016.08.004.
[66] A.K. Mittal, S. Kumar, U.C. Banerjee, Quercetin and gallic acid mediated synthesis of bimetallic (silver and selenium) nanoparticles and their antitumor and antimicrobial potential, J. Colloid Interface Sci. 431 (2014) 194–199, https://doi.org/10.1016/j.jcis.2014.06.030.
[67] V.L.C. Tan, A. Hinchman, R. Williams, P.A. Tran, K. Fox, Nanostructured biomedical selenium at the biological interface (Review), Biointerphases 13 (2018), https://doi.org/10.1116/1.5042693.
[68] T. Chen, Yang, Zhong Tang, Zhang Bai, et al., Surface decoration by Spirulina polysaccharide enhances the cellular uptake and anticancer efficacy of selenium nanoparticles, Int. J. Nanomed. (2012) 835, https://doi.org/10.2147/ijn.s28278.
[69] W.-Y. Qiu, Y.-Y. Wang, M. Wang, J.-K. Yan, Construction, stability, and enhanced antioxidant activity of pectin-decorated selenium nanoparticles, Colloids Surf. B Biointerfaces 170 (2018) 692–700, https://doi.org/10.1016/j.colsurfb.2018.07.003.
[70] K. Anu, G. Singaravelu, K. Murugan, G. Benelli, Green-synthesis of selenium nanoparticles using garlic cloves (allium sativum): biophysical characterization and cytotoxicity on Vero cells, J. Cluster Sci. 28 (2016) 551–563, https://doi.org/10.1007/s10876-016-1123-7.
[71] M. Fernandes, K. RB Singh, T. Sarkar, P. Singh, R. Pratap Singh, Recent applications of magnesium oxide (mgo) nanoparticles in various domains, Advanced Materials Letters 11 (2020) 1–10, https://doi.org/10.5185/amlett.2020.081543.
[72] P. Singh, K.R.B. Singh, R. Verma, J. Singh, R.P. Singh, Efficient Electro-optical characteristics of bioinspired iron oxide nanoparticles synthesized by Terminalia chebula dried seed extract, Mater. Lett. 307 (2022) 131053, https://doi.org/10.1016/j.matlet.2021.131053.
[73] E.P. Figueiredo, J.M. Ribeiro, E.K. Nishio, S. Scandorieiro, A.F. Costa, V.F. Cardozo, et al., New approach for simvastatin as an antibacterial: synergistic effect with bio-synthesized silver nanoparticles against multidrug-resistant bacteria, Int. J. Nanomed. 14 (2019) 7975–7985, https://doi.org/10.2147/ijn.s211756.
[74] S. Mallick, K.R.B. Singh, V. Nayak, J. Singh, R.P. Singh, Potentialities of core@shell nanomaterials for Biosensor Technologies, Mater. Lett. 306 (2022) 130912, https://doi.org/10.1016/j.matlet.2021.130912.
[75] R. Brigelius-Flohé, Selenium compounds and selenoproteins in cancer, Chem. Biodivers. 5 (2008) 389–395, https://doi.org/10.1002/cbdv.200890039.